



Universiteit  
Leiden  
The Netherlands

## **Predictions of bedaquiline and pretomanid target attainment in lung lesions of tuberculosis patients using translational minimal physiologically based pharmacokinetic modeling**

Mehta, K.M.; Guo, T.; Graaf, P.H. van der; Hasselt, J.G.C. van

### **Citation**

Mehta, K. M., Guo, T., Graaf, P. H. van der, & Hasselt, J. G. C. van. (2023). Predictions of bedaquiline and pretomanid target attainment in lung lesions of tuberculosis patients using translational minimal physiologically based pharmacokinetic modeling. *Clinical Pharmacokinetics*, 62(3), 519-532. doi:10.1007/s40262-023-01217-7

Version: Publisher's Version

License: [Creative Commons CC BY-NC 4.0 license](https://creativecommons.org/licenses/by-nc/4.0/)

Downloaded from: <https://hdl.handle.net/1887/3656422>

**Note:** To cite this publication please use the final published version (if applicable).



# Predictions of Bedaquiline and Pretomanid Target Attainment in Lung Lesions of Tuberculosis Patients using Translational Minimal Physiologically Based Pharmacokinetic Modeling

Krina Mehta<sup>1</sup> · Tingjie Guo<sup>1</sup> · Piet H. van der Graaf<sup>1,2</sup> · J. G. Coen van Hasselt<sup>1</sup>

Accepted: 19 January 2023 / Published online: 19 February 2023  
© The Author(s) 2023

## Abstract

**Background** Site-of-action concentrations for bedaquiline and pretomanid from tuberculosis patients are unavailable. The objective of this work was to predict bedaquiline and pretomanid site-of-action exposures using a translational minimal physiologically based pharmacokinetic (mPBPK) approach to understand the probability of target attainment (PTA).

**Methods** A general translational mPBPK framework for the prediction of lung and lung lesion exposure was developed and validated using pyrazinamide site-of-action data from mice and humans. We then implemented the framework for bedaquiline and pretomanid. Simulations were conducted to predict site-of-action exposures following standard bedaquiline and pretomanid, and bedaquiline once-daily dosing. Probabilities of average concentrations within lesions and lungs greater than the minimum bactericidal concentration for non-replicating ( $MBC_{NR}$ ) and replicating ( $MBC_R$ ) bacteria were calculated. Effects of patient-specific differences on target attainment were evaluated.

**Results** The translational modeling approach was successful in predicting pyrazinamide lung concentrations from mice to patients. We predicted that 94% and 53% of patients would attain bedaquiline average daily PK exposure within lesions ( $C_{avg-lesion} > MBC_{NR}$ ) during the extensive phase of bedaquiline standard (2 weeks) and once-daily (8 weeks) dosing, respectively. Less than 5% of patients were predicted to achieve  $C_{avg-lesion} > MBC_{NR}$  during the continuation phase of bedaquiline or pretomanid treatment, and more than 80% of patients were predicted to achieve  $C_{avg-lung} > MBC_R$  for all simulated dosing regimens of bedaquiline and pretomanid.

**Conclusions** The translational mPBPK model predicted that the standard bedaquiline continuation phase and standard pretomanid dosing may not achieve optimal exposures to eradicate non-replicating bacteria in most patients.

## 1 Introduction

Tuberculosis (TB) continues to be a global health challenge. Rifampin and isoniazid are two key first-line antibiotics against *Mycobacterium tuberculosis* (Mtb). Increasing levels and frequency of resistance against rifampin and isoniazid over time necessitated the discovery of new anti-TB antibiotics [1]. Within the last decade, two promising second-line antibiotics, bedaquiline and pretomanid,

### Key Points

It is important to understand the site-of-action tissue distribution of antituberculosis to optimize treatment strategies. We developed and validated a translational minimal physiologically based pharmacokinetic approach that allowed predictions for bedaquiline and pretomanid lung and cavitory lesion exposures.

The model predicted that although current standard dosing of bedaquiline and pretomanid may achieve site-of-action exposures to exhibit bactericidal activity against replicating bacteria, additional treatment optimization may be required for eradication of non-replicating bacteria.

✉ Krina Mehta  
coen.vanhasselt@lacdr.leidenuniv.nl

J. G. Coen van Hasselt  
coen.vanhasselt@lacdr.leidenuniv.nl

<sup>1</sup> Leiden Academic Centre for Drug Research, Leiden University, Leiden, The Netherlands

<sup>2</sup> Certara, Canterbury, UK

were developed as a result of increased efforts to tackle drug-resistant TB [2, 3]. A combination regimen containing bedaquiline, pretomanid, and linezolid (BPaL) showed Mtb clearance (CL) as measured by negative culture status in 90% of patients with drug-resistant TB after 6 months of therapy [4]. BPaL is now recommended for the treatment of rifampin-resistant TB and multidrug-resistant TB patients [1].

Drug exposures at the site of action, within lungs and especially within cavitory lesions, are correlated with bactericidal and sterilizing activities against Mtb. Anaerobic conditions within the necrotic region of the lesion microenvironment, caseum, provide a survival niche for non-replicating but persistent Mtb [5]. Inadequate exposures within cavitory lesions can lead to resistance development. Measuring drug pharmacokinetics (PK) within the lungs and lesions of TB patients usually requires invasive methods to obtain samples and therefore is not readily possible. Preclinical animal models have traditionally been used to evaluate drug penetration at sites of action. These results require accounting for interspecies differences in physiological, pathological, and drug-specific aspects to translate to the patients [6]. Newer methods, such as positron emission tomography (PET) imaging methods, are increasingly being implemented to measure drug penetration at the site of action following intravenous administration of radiolabeled drugs to measure the relative fraction of drug penetration at the site of action [7]. A key benefit of this method is that it can be performed in the patients and as such can allow evaluations of tissue-specific PK with patient-specific covariates.

In silico approaches allow the incorporation of available data for the development of predictive models for optimal decision making. Population PK (PopPK) modeling approaches have been previously applied to quantify the relationship between plasma and lesion PK for several first- and second-line TB antibiotics; however, this approach can only be applied when sites of action measurements are available from patients [8, 9]. Minimal physiologically based PK (mPBPK) models are well suited for translational predictions of the relationship between drug PK in blood plasma and at sites of action. Such models can account for known species-related differences and can incorporate patient covariates and expected interindividual variability and uncertainty in the parameter estimate to allow population simulations. The probability of target attainment (PTA) can then be predicted by defining target attainment to the desired breakpoint based on experimental data [5]. In general, several experimental methods exist to understand drug exposures at the site of action. These methods should be used in combination with in silico approaches to rationally predict overall treatment response in TB patients.

Bedaquiline and its primary metabolite M2 exposures at the current standard dosing regimen (400 mg once daily for 14 days followed by 200 mg three times weekly) have the potential for safety concerns related to QTc interval prolongation and hepatic adverse events [10–12]. Alternative once-daily dosing (200 mg once daily for 8 weeks followed by 100 mg once daily) of bedaquiline is of interest to increase patient adherence to obtain optimal efficacy [12]. Pretomanid has overall acceptable clinical safety profiles; however, pretomanid combined with bedaquiline and linezolid can have additive effects, leading to an increased potential of certain adverse effects [13]. As such, understanding drug exposures within the systemic circulation and at sites of action is crucial to evaluate combination treatment strategies to ensure the attainment of adequate exposures to maximize efficacy, avoid resistance development, and minimize safety issues.

The main objective of this work was to predict bedaquiline and pretomanid lung and lesion exposures in TB patients to understand the PTA and the impact of patient covariates, body weight, and cavity size on PTA. To this end, we developed and validated a translational mPBPK modeling approach that allowed to predict bedaquiline and pretomanid PK at standard and alternative once-daily dosing and calculation of PTA in lungs and lesions using pre-clinical data.

## 2 Methods

A general translational mPBPK framework including lungs and lesions was first developed and validated using available lung PK data in mice and humans for pyrazinamide. The framework was then implemented for the development and assessment of bedaquiline and pretomanid models. Simulations were conducted to predict site-of-action exposures at standard bedaquiline and pretomanid dosing and an alternative bedaquiline dosing. The simulations were then compared against critical concentration estimates to evaluate the effects of body weight and cavity size on lesion PTA.

### 2.1 General Modeling Approach

#### 2.1.1 Minimal Physiologically Based Pharmacokinetic (mPBPK) Model Structure

The model development for all drugs was based on a general mPBPK structural model containing central and lung compartments [14]. The mPBPK models were parameterized using species-specific physiological parameters, such as body weight, cardiac output, lung and other tissue volumes, and volume of blood in systemic circulation [15]. Drug-specific parameters, such as blood-to-plasma ratio and plasma protein

**Table 1** Parameter estimates of bedaquiline, pretomanid, and pyrazinamide mPBPK models

Parameter (units)	Description	Parameter estimate		%RSE	References
		Mice	Humans		
<i>Physiological</i>					
Qc (L/h)	Cardiac output	0.839	312 (for 70 kg)		[15]
Qh (fraction of Qc)	Blood flow to liver	0.161	0.227		
Vliv (fraction of body weight)	Volume of liver	0.0549	0.0549		
Vbl (fraction of body weight)	Volume of blood reservoir	0.077	0.077		
<i>Bedaquiline</i>					
fup (%)	Unbound fraction	0.1	0.1		[27]
BP	Blood-to-plasma ratio	1	1	–	[34]
ka1 (1/h)	Absorption rate from depot1	1.3	1.3	37.8	Estimated
ka2 (1/h)	Absorption rate from depot2	0.00501	0.00501	9.13	
CLint (L/h)	Intrinsic clearance	1.21	60.3	16.7	
KpT	Partition coefficient for tissue compartments	4.45	4.45	15.3	
CLM2 (L/h)	Clearance for M2	0.0119	45.9	13.6	
KpTM2	Partition coefficient for tissue compartments for M2	9.54	9.54	18.4	
R <sub>le</sub>	Penetration ratio for lung lesion	11	11	10.7	
R <sub>ul</sub>	Penetration ratio for uninvolved lungs	10.2	10.2	10.9	
R <sub>le</sub> M2	Penetration ratio for lung lesion for M2	88.4	88.4	5.72	
R <sub>ul</sub> M2	Penetration ratio for uninvolved lungs for M2	88.8	88.8	5.53	
frc	Fraction going through fast absorption (depot1)	0.609	0.609	11.9	
IIV for ka1, ka2, CLint, CLM2, KpT, and KpTM2 (%)	Log-normally distributed random variability in bedaquiline parameters for human simulations	–	40	–	
MBC <sub>NR</sub>	Minimum bactericidal concentration for non-replicating bacteria (ng/mL)	–	17760	–	[5]
MBC <sub>R</sub>	Minimum bactericidal concentration for replicating bacteria (ng/mL)	–	5500	–	[5]
MIC range	Minimum inhibitory concentration range (ng/mL)	–	600–2500	–	[40]
<i>Pretomanid</i>					
BP	Blood-to-plasma ratio	1.65	1.65		[13]
ED50 (mg)	Dose at which bioavailability is 50% of the maximum, which was assumed to be 1	7.59	554	14.8	Mice estimated, humans [41]
k <sub>a</sub> (1/h)	Absorption rate	0.3	0.3	23.3	Estimated
CL (L/h)	Apparent clearance	0.016	4.42	3.78	
KpT	Partition coefficient for tissue compartment 1	36.3	36.3	3.77	
FT1	Fraction going to tissue compartment 1	0.97	0.97	9.72	
KpT1	Partition coefficient for tissue compartment 2	0.483	0.483	14	
R <sub>le</sub>	Penetration ratio for lung lesion	1.05	1.05	145	
R <sub>ul</sub>	Penetration ratio for uninvolved lungs	1.75	1.75	13.8	
IIV for k <sub>a</sub> , ED50, CL, KpT, and KpT2 (%)	Log-normally distributed random variability in pretomanid parameters for human simulations	–	40	–	
MBC <sub>NR</sub>	Minimum bactericidal concentration for non-replicating bacteria (ng/mL)	–	6300	–	[13]
MBC <sub>R</sub>	Minimum bactericidal concentration for replicating bacteria (ng/mL)	–	20	–	[13]

**Table 1** (continued)

Parameter (units)	Description	Parameter estimate		%RSE	References
		Mice	Humans		
MIC range	Minimum inhibitory concentration range (ng/mL)	–	8–4000	–	[13]
<i>Pyrazinamide</i>					
BP	Blood-to-plasma ratio	0.79	0.79	–	[42]
ka (1/h)	Absorption rate	0.30	0.05 <sup>a</sup>	7.25	Estimated
CL (L/h)	Apparent clearance	0.014	3.5	3.04	
R <sub>le</sub>	Penetration ratio for lung lesion	1.37	1.37	52.2	
R <sub>ul</sub>	Penetration ratio for uninvolved lungs	0.85	0.85	102	
IIV for ka and CL (%)	Log-normally distributed random variability in pyrazinamide parameters for human simulations (%)	–	40	–	

Estimated residual errors in model fitting to mice data were as follows: combined bedaquiline plasma, liver, and M2 plasma = proportional 43%; bedaquiline and M2 lesions and lungs = proportional 53%; pretomanid plasma = proportional 12%; pretomanid lesions = proportional 6% and additive 2.24 ng/mL; pretomanid lungs = proportional 12% and additive 0.239 ng/mL; pyrazinamide combined plasma, lungs, and lesions = proportional 35%. Residual errors were not included in the human simulations

*mPBPK* minimal physiologically based pharmacokinetic, *RSE* relative standard error

<sup>a</sup>Allometrically scaled from mice to humans using an exponent of – 0.25

binding were obtained from the literature. Other drug-specific parameter estimates, such as absorption rates, partition coefficients, and apparent CL were estimated using the data from PK studies in mice (electronic supplementary material [ESM] S1). Additional structural components were evaluated in a stepwise manner as suggested by the available data and prior knowledge. For instance, plasma concentrations of the primary metabolite of bedaquiline, M2, are of importance due to its relevance to safety concerns [16, 17]. Therefore, mechanistic representation of the metabolism of bedaquiline to M2 was described using a liver compartment represented by the well-stirred liver model. Although *in vitro* and mice experimental studies have demonstrated lower anti-Mtb activity of M2 compared with bedaquiline, its site-of-action exposures can be useful to evaluate its overall impact on bacterial load in TB patients using PK/pharmacodynamic (PD) models; therefore, M2 lung and lesion compartments were included in the model and the relevant parameters were estimated using mice M2 lung and lesion data. Different absorption models, i.e., multiple-site absorption, transit compartment absorption model, and dose-dependent bioavailability, were evaluated.

Drug uptake in lung lesions and uninvolved lungs was described using the effect compartment structural model as described previously [18]. Rates of drug transport between systemic circulation and lesion and uninvolved lung compartments were described by blood flow rates to these compartments calculated based on the approximate lesion and total lung volumes. The volume of lesions and uninvolved lungs were calculated based on the mean total lesion volume reported in the literature for cavitary TB patients and species-specific total lung volumes [19].

$$d/dt(C_i) = k_i \times (C_{bld} \times R_i - C_i)$$

$$k_i = Q_c / V_i$$

$$V_i = V_{lung} \times V_{Fi}$$

Here, *i* represents compartments, i.e., lesions or uninvolved lungs; *C<sub>i</sub>* represents drug concentration in the respective compartment; *C<sub>bld</sub>* is drug concentration in systemic circulation; *k<sub>i</sub>* is the transfer rate constant to the respective compartment; *R<sub>i</sub>* is the penetration ratio for the respective compartment; *Q<sub>c</sub>* is cardiac output; *V<sub>lung</sub>* is the total volume of lungs; *V<sub>Fi</sub>* is the fractional volume of the respective compartment; and *V<sub>i</sub>* is the volume of the respective compartment. Mean volume of lesions (*V<sub>le</sub>*) was assumed to be 0.0216, calculated based on the mean total lesion volume, approximately 14 mL, reported in the literature for cavitary TB patients [19]. *V<sub>ul</sub>* was calculated as 1-*V<sub>le</sub>*.

## 2.2 Translation of the mPBPK Models to Tuberculosis Patients

The mice mPBPK models developed using mice data were scaled to TB patients considering physiological differences between the species. Physiological parameters such as cardiac output and volumes of compartments for humans were obtained from the literature [15]. A drug-specific parameter, CL, was scaled from mice to humans using a previously known allometric exponent of 0.75 for CL [20]. For the absorption rate parameter (*ka*), plasma PK predictions using

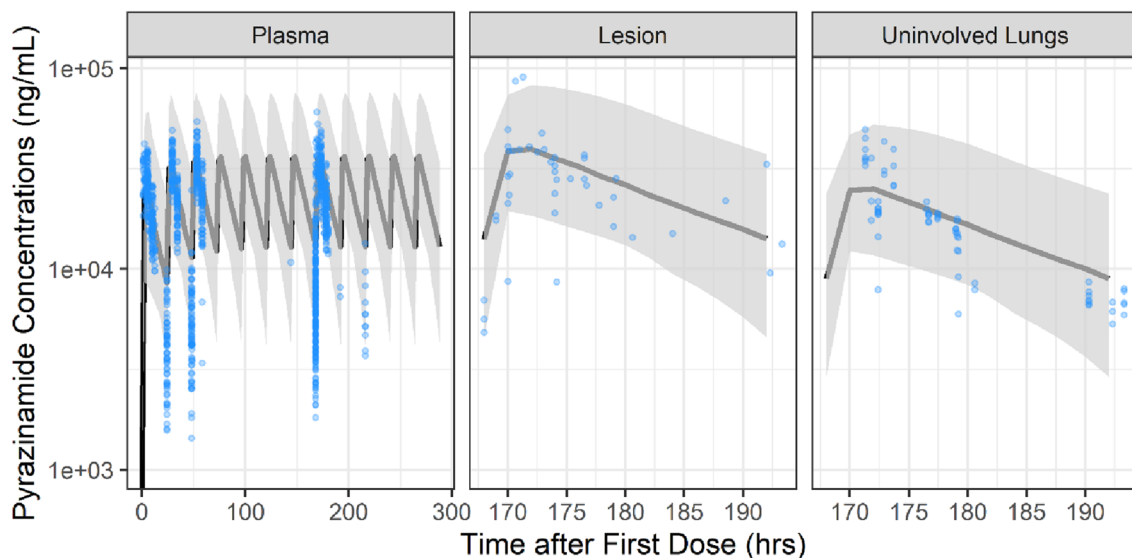


**Fig. 1** Evaluation of the modeling approach using pyrazinamide PK profiles in TB patients. Pyrazinamide model predictions showed good agreement with the observed data from TB patients, suggesting the reliability of our mPBPK framework for other TB antibiotics. Pyrazinamide 1500 mg oral dosing was simulated and compared against observed data from plasma, lungs, and lesions of TB patients [22, 28, 38] accessed through TB-PACTS. Both observed data and simula-

tions for lungs and lesions represent one dosing cycle at steady state. Blue points represent observed data, solid grey line represents the median of the simulations, and shaded grey area represents the 95% PI of the simulations. *PK* pharmacokinetic, *TB* tuberculosis, *mPBPK* minimal physiologically based pharmacokinetic, *TB-PACTS* platform for aggregation of clinical TB studies, *PI* prediction interval

the model scaling with an allometric exponent of  $-0.25$  and models without any scaling were compared with the observed data for each drug prior to selecting whether or not to scale  $k_a$  from mice to humans. The same estimated partition coefficients and penetration ratios for each drug and compartment from mice were assumed for TB patients. To simulate a standard TB population, body weights for 500 virtual patients were sampled from the body weight distribution from clinical trial data (ESM S1). Cavity presence or absence was also sampled from observed distribution from the clinical trials dataset. For virtual patients with a cavity, cavity size was simulated considering normal distribution using reported mean and standard deviation of total lesion volume in cavitary TB patients [19]. Log-normally distributed between-subject variability of 25–40% was added in the relevant parameters. To account for uncertainty in the parameter estimates, 50 trials with the estimated relative standard error (RSE) were simulated for each of the 500 virtual patients. All parameters for both mice and humans, including variability and RSE, are presented in Table 1.

### 2.3 Evaluation of the Modeling Approach Using Pyrazinamide Data

An external evaluation of the predictability of our overall approach was performed using pyrazinamide plasma, lungs, and lesions PK data from mice and TB patients [21, 22]. Therefore, preclinical mice data for pyrazinamide

were digitized from the literature [21] and were used in pyrazinamide mPBPK model development. Next, pyrazinamide clinical studies data were compiled from the literature [22] and from the Platform for Aggregation of Clinical TB Studies (TB-PACTS; <https://c-path.org/programs/tb-pacts/>). Simulated lesion and uninvolved lung PK profiles of pyrazinamide were compared against available observed data in TB patients [22] (ESM S1).

### 2.4 Bedaquiline and Pretomanid Model Development and Assessment

Bedaquiline and pretomanid model development was conducted using PK data from mice. PK data from plasma, liver, and lungs, including both lung lesions and uninvolved lungs of mice for bedaquiline and its primary metabolite M2, were extracted from the literature [21, 23]. Plasma PK data from mice treated with oral pretomanid were also digitized [24]. PK concentrations from PET imaging of plasma, lung lesions, and uninvolved lungs of mice that were administered a single intravenous dose of radioactive  $^{18}\text{F}$ -pretomanid were also digitized [25]. The PK concentrations obtained using PET imaging were represented as relative units (i.e., percentage of injected dose per millimeter [%ID/mL]); therefore, relevant doses were set to 100% in the analysis dataset. Model development was performed using the mPBPK generic structure

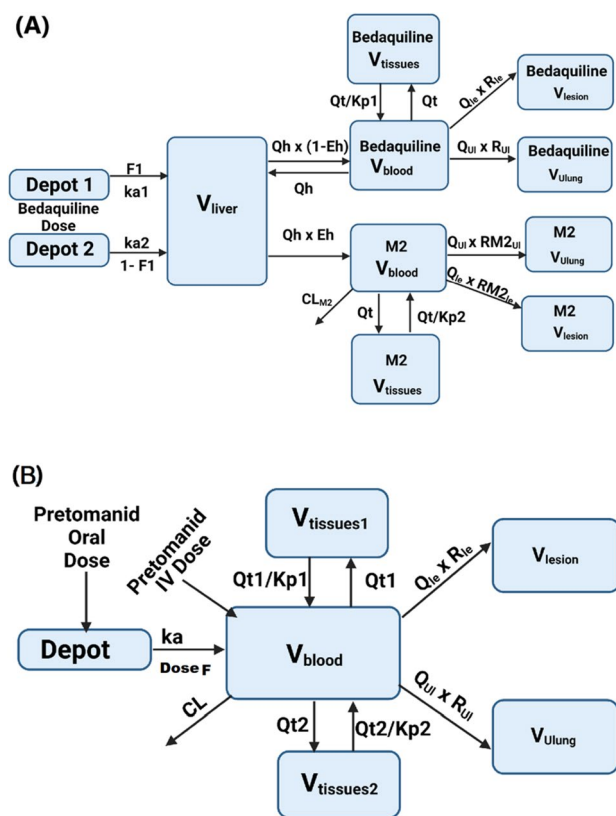


**Fig. 2** Final model structures for **a** bedaquiline and **b** pretomanid. The mPBPK models for bedaquiline and pretomanid contain the relevant compartments, including lungs and lung lesions. Blood, liver, lungs, and lung lesions are represented by their volumes and the rest of the body is lumped into tissue compartment(s). Compartments are connected with each other by blood flows.  $CL$  plasma clearance,  $DoseF$  dose-dependent bioavailability,  $Eh$  hepatic extraction ratio,  $F1$  bioavailability of depot1,  $ka1$  absorption rate from depot1,  $ka2$  absorption rate from depot2,  $Kp$  partition coefficient for tissue compartments,  $Qh$  blood flow to liver,  $Qle$  blood flow rate to lung lesions,  $Qt$  blood flow to tissues,  $QUL$  blood flow rate to unaffected lungs,  $R_{le}$  penetration ratio for lung lesion,  $R_{UL}$  penetration ratio for unaffected lungs,  $V_{blood}$  volume of blood reservoir,  $V_{liver}$  volume of liver,  $V_{tissues}$  volume of the tissue compartment, *mPBPK* minimal physiologically based pharmacokinetic, *IV* intravenous

as described above. Evaluations of additional drug-specific components were guided by data and the parameters were estimated using a model fitting to mice data. Model development and final model selection were guided by objective function value (OFV), the goodness-of-fit (predictions vs. observed) plots, physiological plausibility of parameter estimates, and precision (RSE) of the estimates.

Assessment of bedaquiline and pretomanid mice to human translated models was conducted using PK data from TB patients. Individual-level PK, body weight, and cavity presentation data from various clinical studies were retrieved from the TB-PACTS database. Data from relevant dose levels and clinical studies were compiled for bedaquiline and pretomanid. Simulated plasma PK profiles for

bedaquiline and pretomanid in TB patients were compared against observed data to evaluate the translated mPBPK model performance in TB patients. No PK data on lesions or uninvolved lungs were available from human subjects for bedaquiline or pretomanid. Local sensitivity analysis was conducted to evaluate the impact of the parameters on steady-state plasma drug exposure and was examined by introducing 10% variation in the parameters one at a time and running the simulations for 50 times.

## 2.5 Pharmacokinetics and Target Attainment Predictions of Bedaquiline and Pretomanid at the Site of Action

Predictions of bedaquiline and pretomanid exposures in the lesions and uninvolved lungs were performed for 500 virtual humans using the body weight and cavity volume distributions from TB patients using the final translated mPBPK models (Table 1). Bedaquiline simulations included currently approved oral dosing of 400 mg once daily for 14 days followed by 200 mg three times weekly. The alternative bedaquiline dosing regimen included in the simulations was 200 mg once daily for 8 weeks followed by 100 mg once daily. Pretomanid simulations included oral dosing of 200 mg once daily. Plots of the predicted lesions and uninvolved lungs PK and drug exposure matrices were prepared. Next, predicted bedaquiline and pretomanid concentrations and exposures at the site of action following either standard or alternative bedaquiline or standard pretomanid dosing were compared against critical concentration estimates based on *in vitro* experiments obtained from the literature. The range for bedaquiline and pretomanid minimum inhibitory concentrations (MICs) for multidrug-resistant (MDR) TB strains, minimal bactericidal concentrations for replicating bacteria ( $MBC_R$ ), and minimal bactericidal concentrations for non-replicating bacteria ( $MBC_{NR}$ ) were obtained from the literature (Table 1) [5, 26]. Plots of predicted PK exposures within lesions and lungs were plotted and compared against the MDR-TB MIC range,  $MBC_R$ , and  $MBC_{NR}$  for both drugs. Attainment of target exposures in the lesions was defined as average daily PK exposure within lesions ( $C_{avg-lesion}$ )  $>$   $MBC_{NR}$  to ensure bactericidal activity against persisting, non-replicating bacteria. Body weight and cavity size from the virtual patient population were binned and PTA was calculated for each bin.

## 2.6 Software

All analyses were conducted in R (R for Windows, v4.1; <https://www.r-project.org/>) using RStudio (RStudio, v1-554; [www.rstudio.com/](http://www.rstudio.com/)). Data management and plotting were performed using the tidyverse package, and parameter optimization and model simulations were conducted using the

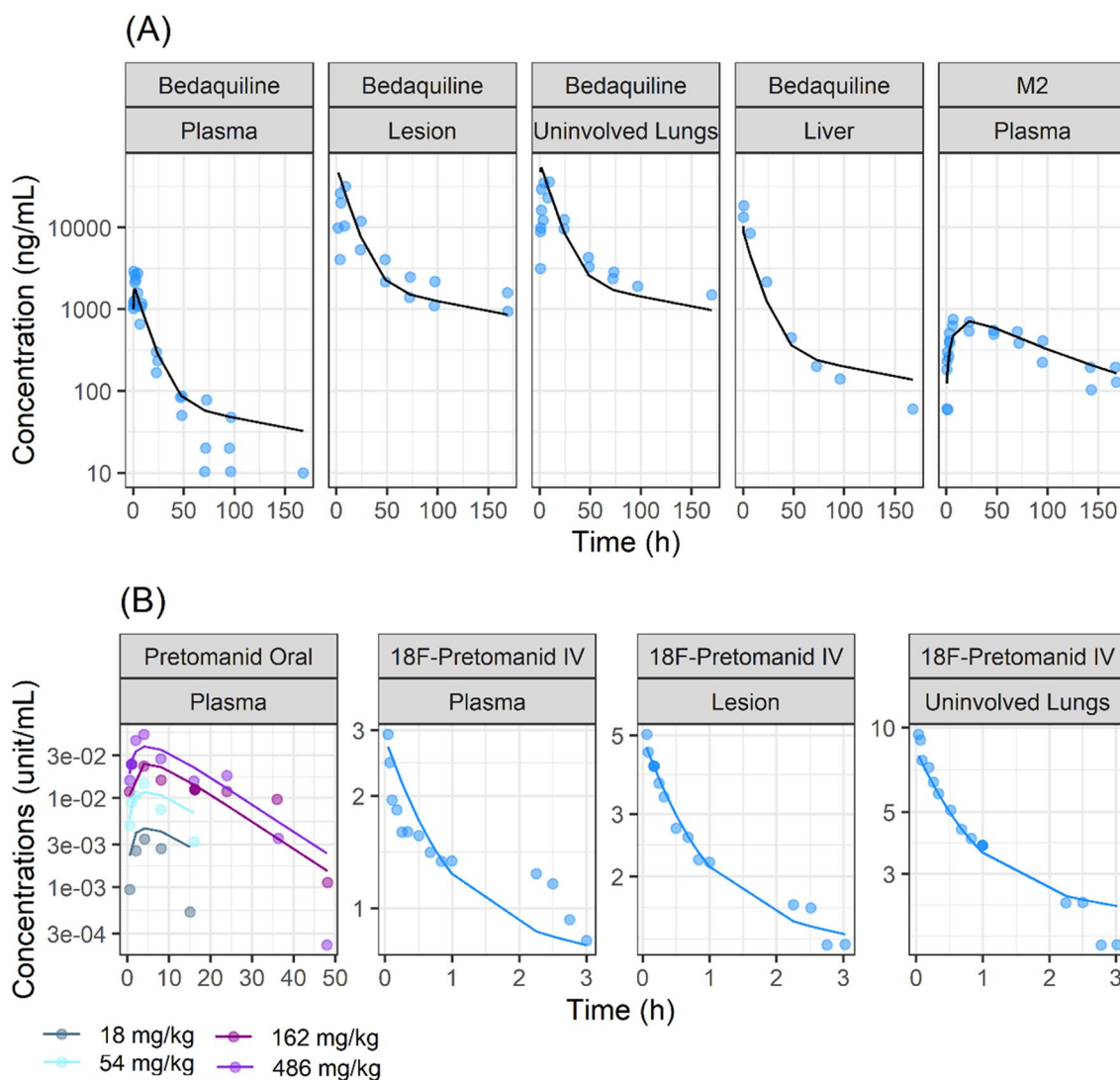


**Fig. 3** Predicted versus observed PK profiles in mice for **a** bedaquiline and **b** pretomanid. The model predictions for plasma, lungs, and lesions for bedaquiline and pretomanid agreed well with the observed data for mice. Bedaquiline 25 mg/kg was administered orally [21], and pretomanid was administered orally at varying doses between 18 and 486 mg/kg [24, 25]. Radioactive 18F-pretomanid was adminis-

tered intravenously and the percentage of the injected dose was measured in plasma, lungs, and lesions of mice. Blue points represent observed data and black line represents model fit predictions. %ID percentage of injected dose, pretomanid concentrations for oral dosing units = ng/mL, 18F-pretomanid concentrations for IV dosing = %ID/mL, PK pharmacokinetic, IV intravenous

nlmixr and RxODE packages. Final model codes are provided in ESM S2.

### 3 Results

#### 3.1 Evaluation of the Modeling Approach Using Pyrazinamide Data

The pyrazinamide mPBPK model was first developed using mice PK data to evaluate the predictability of our translational mPBPK approach. Pyrazinamide plasma, lung lesions, and uninvolved lungs PK data from mice were best described

by the mPBPK structural model with first-order absorption and first-order elimination (ESM S3). The addition of a tissue compartment and evaluations of other absorption models did not improve the model fit. The parameters describing plasma PK were estimated with good precision (RSE < 20%), and the parameters  $R_{le}$  and  $R_{ul}$  were associated with an RSE of 52% and 102%, respectively (Table 1). The scaled mPBPK model appropriately described pyrazinamide plasma, lung lesion, and uninvolved lung concentrations at steady-state from TB patients using allometric exponents of -0.25 for  $k_a$  and 0.75 for CL (Table 1, Fig. 1). Overall, the pyrazinamide model predictions showed good agreement with the observed data from mice and TB patients,



**Table 2** Observed versus predicted exposure comparison for bedaquiline and pretomanid at standard dosing at steady state

Exposure metric (mg/L)	Bedaquiline 400 mg once daily		Bedaquiline 200 mg thrice weekly		Pretomanid 200 mg once daily	
	Observed [27]	Predicted	Observed [27]	Predicted	Observed [13]	Predicted
$C_{avg_{ss}}$	2.696 (0.865) <sup>a</sup> 1.371 (0.529) <sup>b</sup>	3.24 (0.497)	0.584 (0.197)	0.68 (0.108)	1.26 (0.16)	1.06 (0.143)
$C_{max_{ss}}$	5.502 (2.965) <sup>a</sup> 2.763 (1.185) <sup>b</sup>	6.29 (1.45)	1.267 (0.435)	1.57 (0.404)	1.7 (0.29)	3.06 (0.61)
$C_{min_{ss}}$	1.448 (0.437) <sup>a</sup> 0.728 (0.257) <sup>b</sup>	1.07 (0.322)	0.356 (0.170)	0.174 (0.062)	0.5 (0.08)	0.149 (0.06)

All values are expressed as mean (standard deviation)

$C_{avg_{ss}}$  average concentration at steady state,  $C_{max_{ss}}$  maximum concentration at steady state,  $C_{min_{ss}}$  minimum concentration at steady state, *MDR* multidrug-resistant, *TB* tuberculosis

<sup>a</sup>Drug-susceptible TB patients

<sup>b</sup>MDR-TB patients

suggesting the reliability of our translational mPBPK approach for other TB antibiotics.

### 3.2 Model Development and Assessment for Bedaquiline and Pretomanid

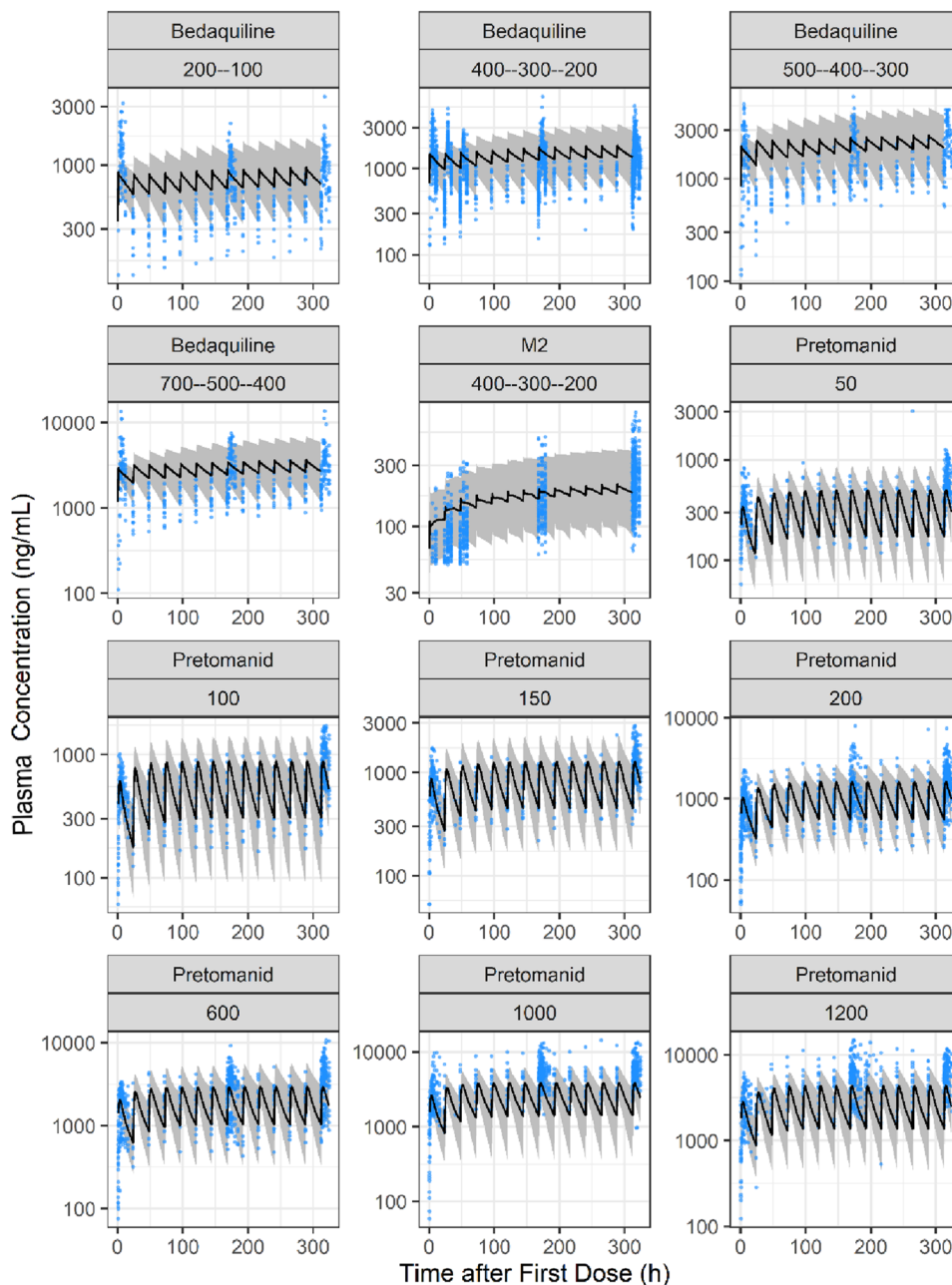
Bedaquiline and M2 PK data from plasma, liver, lung lesions, and uninvolved lungs of *Mtb*-infected mice was best described by the mPBPK structural model containing two parallel first-order absorptions that are in alignment with prior bedaquiline PopPK models, parent-metabolite well-stirred liver compartment, tissue compartments for both bedaquiline and M2, first-order elimination of M2, and lung lesion and uninvolved lung compartments (Fig. 2a). Other components that were evaluated but did not provide improvements in the model fit included only one first-order absorption, transit compartment absorption, and saturable conversion of bedaquiline to M2. All parameters were estimated with reasonable precision (RSE < 40%) (Table 1), and the model predictions showed good agreement with the observed data in mice (Fig. 3a, ESM S4a).

Slight underpredictions of bedaquiline and overpredictions of M2 plasma concentrations were noted when the mPBPK model was directly scaled from mice to humans using only allometric scaling. This was assumed to be due to the species difference between mice and humans in bedaquiline and M2 metabolism and has been previously noted [23, 27]. To account for this difference, calibration of two parameters, intrinsic CL (CL<sub>int</sub>) and CL of M2 (CL<sub>M2</sub>) was performed by fitting to median rich concentration-time profiles from TB patients for one dose group (400 mg on day 1, 300 mg on day 2, and 200 mg days 3–14) [28]. The updated model predicted both bedaquiline and M2 plasma concentration-time profiles well for all dose groups in the dataset (Table 2, Fig. 4). With a 10% or 50% variation in parameter

estimates, the mean sensitivity index was low (between – 1 and 1) for both bedaquiline and M2, with the exception of absorption rate of depot2 (ka<sub>2</sub>), which showed high sensitivity for both bedaquiline and M2 plasma concentrations (ESM S6). Overall, this mPBPK model for bedaquiline and M2 was deemed reliable for predictions of exposures at the site of action, within lung lesions, in TB patients.

Pretomanid oral absorption was best described by a first-order absorption model with dose-dependent bioavailability. Transit compartment absorption was evaluated but did not provide improvements in the model fits. Pretomanid plasma PK after oral dosing, and F18-pretomanid plasma, lung lesion, and uninvolved lung PK after F18-pretomanid intravenous dosing were best described by the mPBPK structural model with two tissue compartments and first-order elimination (Fig. 2b). All parameters were estimated with reasonable precision (RSE < 45%), except that R<sub>1e</sub> was estimated, with an RSE of 145% due to limited lesion PK data (Table 1). Overall, the model predictions showed good agreement with the observed data from mice following either F18-pretomanid intravenous dosing or pretomanid oral dosing (Fig. 3b). Reasonable agreement between observed data and scaled-up human model predictions was noticed for plasma PK data for pretomanid from TB patients, although some underpredictions were noted at 1000 mg and 1200 mg doses (Table 2, Fig. 4). With a 10% change in parameter estimates, the sensitivity for key pretomanid PK parameters was relatively low (between – 2.5 and 2.5), with the exception of partition coefficient for tissue compartment 1 (kpT1), which showed moderate sensitivity for pretomanid plasma concentrations. This further supported the reliability of the model (ESM S6). Overall, the mPBPK model for pretomanid was deemed reliable for prediction of exposures at the site of action, within lung lesions, following clinically relevant doses in TB patients.

**Fig. 4** Predicted and observed plasma PK profiles in TB patients for bedaquiline, M2, and pretomanid. The model predictions for plasma bedaquiline, M2, and pretomanid agreed well with the observed data for TB patients from clinical trials at various doses [28, 39]. Blue points represent the observed data, solid grey line represents the median of the simulations, shaded grey area represents the 95% PI of the simulations. Panel titles represent bedaquiline or pretomanid doses in milligrams. Bedaquiline was administered as an increasing daily dose, i.e., panel 1 represents a group that received 200 mg on day 1 and 100 mg on day 2 onwards. PK pharmacokinetic, TB tuberculosis, PI prediction interval



### 3.3 Pharmacokinetics and Target Attainment Predictions of Bedaquiline and Pretomanid at the Site of Action

The simulations suggested good penetration for bedaquiline in both lung lesions and uninvolved lungs (Fig. 5a). The predicted bedaquiline median (95% prediction interval) lesion-to-plasma ratio was 11.0 (10.5–11.4) and uninvolved lungs-to-plasma ratio was 10.2 (9.8–10.5). Bedaquiline lesions and uninvolved lung concentrations were predicted to remain above the MIC range observed for MDR-TB isolates at standard dosing and alternative

once-daily dosing [26]. Bedaquiline lesion and uninvolved lung concentrations were predicted to be slightly above  $MBC_R$  for all virtual patients throughout the treatment period during the extensive phase of standard dosing and alternative once-daily dosing (Fig. 5a) [5, 26]. At standard bedaquiline dosing, 94% of virtual patients were predicted to have  $C_{avg-lesion} > MBC_{NR}$  after extensive dosing (400 mg once daily) for the first 14 days of treatment, but < 5% of virtual patients were predicted to have  $C_{avg-lesion} > MBC_{NR}$  throughout the continuation phase of treatment when dosing was reduced to 200 mg three times weekly. At alternative once-daily bedaquiline dosing, a total of 86%

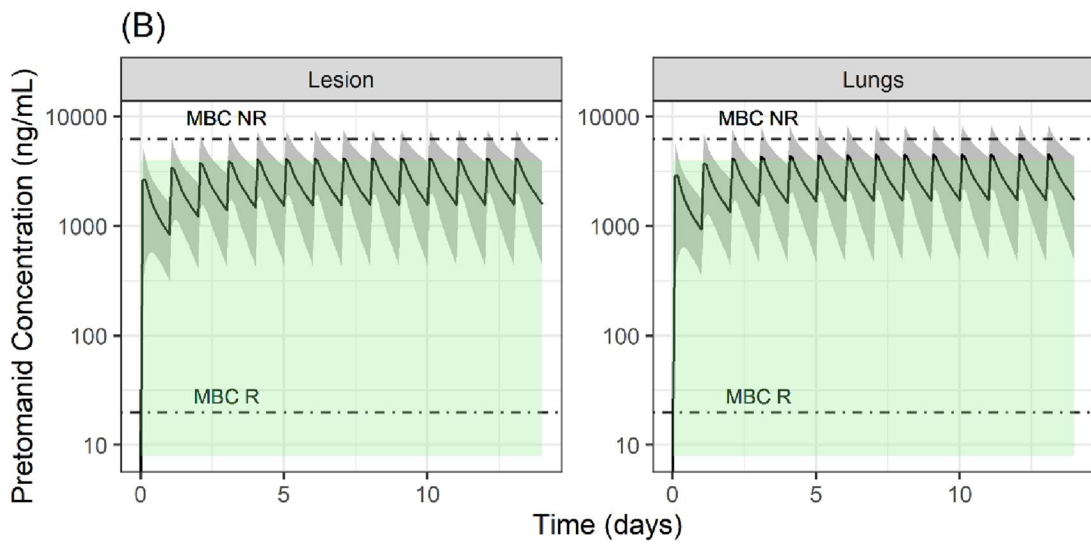
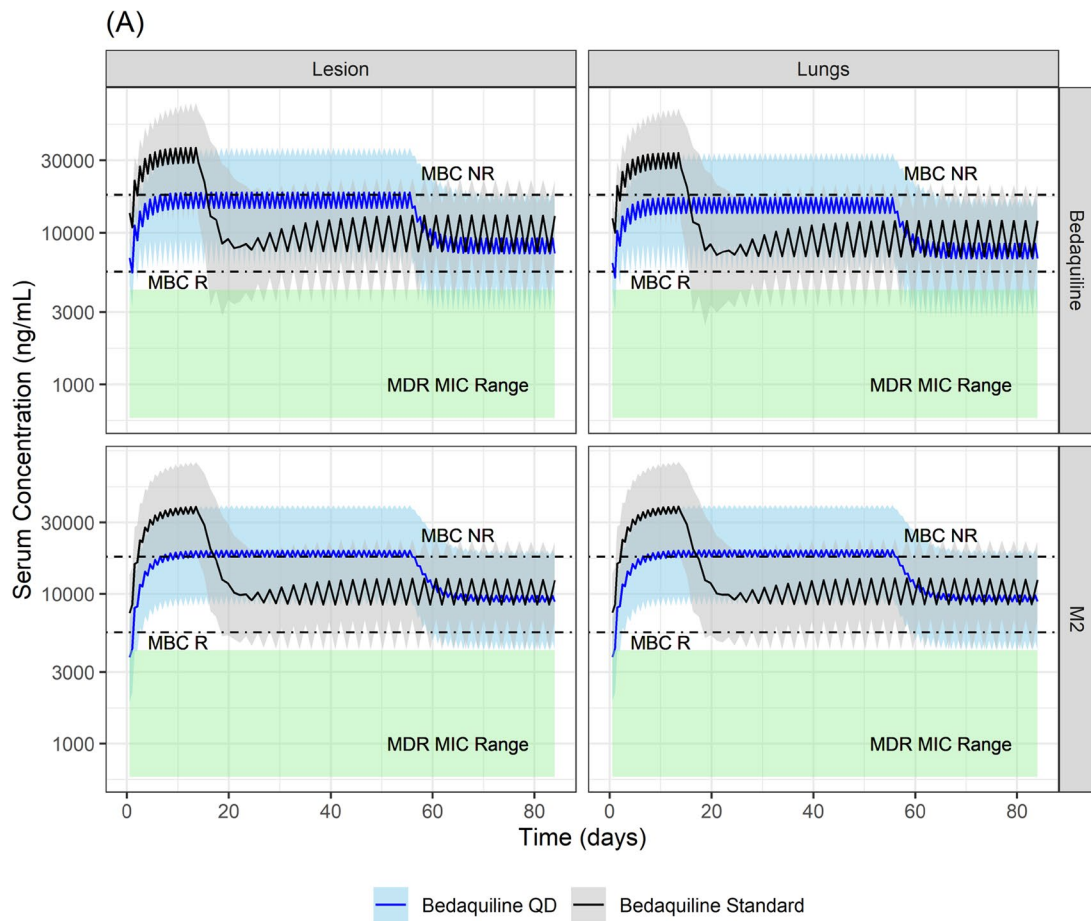


**Fig. 5** Simulated PK profiles at sites of action in TB patients. **a** Bedaquiline standard and once-daily dosing, and **b** pretomanid. Bedaquiline standard dosing included 400 mg once daily for 14 days followed by 200 mg 3 days a week. Bedaquiline once-daily dosing included 200 mg once daily for 8 weeks followed by 100 mg once daily. Pretomanid dosing included 200 mg once daily. The model predicted that lung and lesion concentrations of bedaquiline and pretomanid would remain above the MIC (for rifampin and/or isoniazid drug-resistant TB strains) and  $MBC_R$  at current clinically relevant doses. Although it was predicted that 94% and 53% of patients would achieve target exposures at standard and alternative once-daily bedaquiline dosing, respectively, it should be noted that alternative once-daily dosing provides higher target attainment for a longer duration (2 vs. 8 weeks). M2 target attainment was predicted to be slightly higher than those of bedaquiline. It should be noted that M2  $MBC$  and MICs were assumed to be the same as those of bedaquiline [40]. Blue or black lines represent the median of the simulations and the shaded blue or grey area represents the 95% PI of the simulations.  $MIC$  minimum inhibitory concentration,  $MDR$  multidrug-resistant tuberculosis,  $MBC_R$  minimum bactericidal concentrations for replicating bacteria,  $MBC_{NR}$  minimum bactericidal concentrations for non-replicating bacteria.  $PK$  pharmacokinetic,  $TB$  tuberculosis,  $PI$  prediction interval,  $QD$  once daily

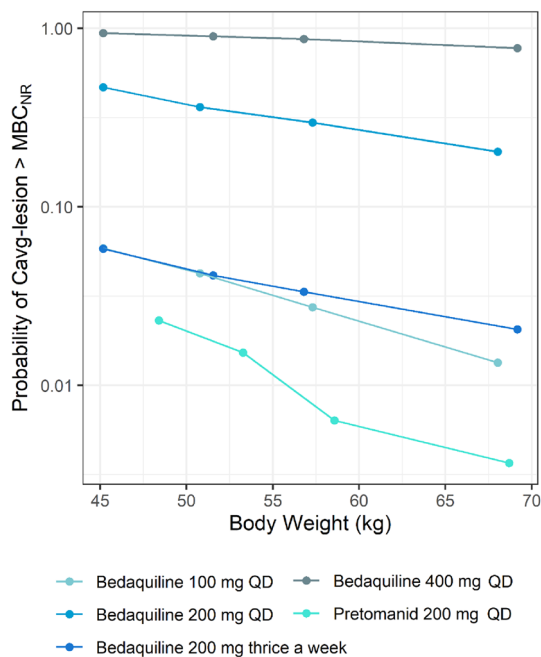


**Fig. 6** Predicted probability of average bedaquiline concentrations above  $MBC_{NR}$  in TB patients, by body weight. Body weight was predicted to have an impact on lesion PTA. PTA was defined as  $Cavg\text{-lesion} > MBC_{NR}$ . PTAs were calculated at steady-state for each dosing group.  $MBC_{NR}$  minimum bactericidal concentrations for non-replicating bacteria,  $TB$  tuberculosis,  $PTA$  probability of target attainment,  $Cavg\text{-lesion}$  average daily PK exposure within lesions,  $MBC_{NR}$  minimum bactericidal concentration for non-replicating bacteria,  $QD$  once daily

of virtual patients were predicted to have  $Cavg\text{-lesion} > MBC_{NR}$  during the extensive phase (200 mg once daily) for the 8 weeks of treatment, but  $< 5\%$  of virtual patients were

predicted to have  $Cavg\text{-lesion} > MBC_{NR}$  throughout the continuation phase of treatment when dosing was reduced to 100 mg once daily. The simulations also suggested relatively similar M2 exposures at the site of action as those of bedaquiline (Fig. 5). Simulated plasma M2 concentrations were below the reported M2  $EC_{50}$  concentrations for QTcF prolongation for 83% of virtual patients during the extensive phase of standard bedaquiline treatment, and for all virtual patients during the continuation phase of standard bedaquiline and both phases of alternative once-daily dosing (ESM S4b). It should be noted that although the PTA is higher with bedaquiline standard dosing during the extensive phase, the period of extensive phase in standard dosing versus alternative once-daily dosing is shorter (2 vs. 8 weeks), which may have a large impact on overall efficacy. The probability of  $Cavg\text{-lesion} > MBC_{NR}$  was predicted to increase with an increase in body weight for both dosing scenarios (Fig. 6). Cavity size was predicted to not affect the attainment of average lesion concentrations above  $MBC_{NR}$ .

The pretomanid predicted median (95% prediction interval) lesion-to-plasma ratio was 2.6 (2.5–2.8) and uninvolved lung-to-plasma ratio was 2.9 (2.7–3.1) [Fig. 5b]. Predicted lesion concentrations after pretomanid 200 mg daily dosing were predicted to remain above the pretomanid MIC range observed for MDR-TB isolates for 18% of virtual patients [13]. Pretomanid lesions and uninvolved lung concentrations were predicted to remain well above the  $MBC_R$  for all patients. Less than 1% of patients were predicted to have pretomanid  $Cavg\text{-lesion} > MBC_{NR}$  (Fig. 5b) [13].

## 4 Discussion

In this work, we developed translational mPBPK models for bedaquiline- and pretomanid-containing lungs, including cavitory lesion compartments, using physiological parameters describing blood flows and volumes of lesions and uninvolved lungs. The mPBPK models adequately described plasma, lungs, and lesions PK data from mice, while the translational mPBPK models adequately described dose-ranging plasma PK data from TB patients. The mPBPK models allowed predictions of bedaquiline and pretomanid exposures and target attainment in the lungs and lesions of TB patients.

One of the concerns against the newer antibiotics bedaquiline and pretomanid is the development of resistance [29]. A key mechanism of resistance development against antibiotics includes a subpopulation of *Mtb*, persisters, developing phenotypic tolerance against the drugs without genetic mutations. This process is reversible; however, suboptimal drug exposures within cavitory lesions where persisters dwell allow them to survive. This eventually allows *Mtb* strains to develop

genotypic mutation and allow replication of genetically resistant strains against antibiotics [30]. As such, it is crucial to optimize therapeutic strategies to eliminate the non-replicating persistent Mtb population during the treatment phase. Our mPBPK models can be combined with various types of experimental *in vitro* and *in vivo* bacterial-kill dynamics and resistance development data to construct mechanistic PK/PD models that can be used to further evaluate optimal strategies against Mtb, especially against persisters within lesions [31].

Our predictions suggested that PTA decreases with an increase in patients' body weight for both bedaquiline and pretomanid. The current dosing regimen for bedaquiline is associated with safety risks of QTcF prolongation and hepatic adverse events; therefore, an increase in bedaquiline dosing may not be a viable approach for all patients. Further efficacy and safety evaluations of bodyweight-based dose optimization for bedaquiline may be useful. The model also captured the PK of the bedaquiline metabolite M2 within plasma and at the site of action. To further evaluate the contribution of M2 on Mtb CL using the developed mPBPK framework, M2-specific PD parameters, such as derived in an *in vitro* experiment, would be required. Model-informed precision dosing approaches can be employed to ensure maximum risk-benefit balance for most patients considering totality of information [32, 33]. The current dosing regimen for pretomanid is considered to be well tolerated. The mechanistic PK/PD model can be used to predict the effects of alternative dosing of pretomanid in combination with bedaquiline and/or other antibiotics on CL of persisting Mtb from lesions.

Previously, standard compartmental models combined with effect compartment structural models or whole-body PBPK modeling combined with mechanistic lung models have been developed for mostly first-line TB antibiotics [8, 9, 34]. Middle-out approaches, such as mPBPK models, allow the balance between empirical compartmental models and rigorous whole-body PBPK models [35]. Our mPBPK model construct included standard physiological parameters, such as blood flow rates and volume for lungs. A key component of our structural model is the parameter describing flow rates to lesions, which were calculated based on total blood flow rates and volume fraction of cavitary lesions. As such, this approach suggests a simple technique to evaluate the impact of cavitary lesion size on target exposure attainment within lesions for anti-TB agents. Our simulations suggested no significant impact of total lesion volume on PTA within lesions for bedaquiline and pretomanid given other variability and uncertainty in the parameters that were estimated using limited preclinical data. Additional model-based analyses using our structural model and longitudinal PET imaging data from lesions of varying sizes from TB patients [7] may allow further insights into understating the impact of cavity size on bedaquiline and pretomanid target attainment within lesions to further optimize treatment strategies.

*In vitro* experimental evaluations of MIC and MBC values for antimicrobials are usually performed using free drug. As such, the role of plasma protein binding may be important for *in vitro/in vivo* response comparisons if plasma drug concentrations are used for predictions of response *in vivo*. Generally, only unbound drug from the systemic circulation is available for diffusion into the tissues. Both bound and unbound drug can penetrate the tissues via active transport; however, as distribution equilibrium is achieved, unbound plasma and unbound tissue concentrations reach equilibrium [36, 37]. The previously described empirical model structure for tissue penetration that was fitted to the observed lung and lesion concentration data allows estimation of lung and lesion distribution parameters relative to plasma drug concentrations, and may empirically account for the contributions of the plasma protein binding [8, 18]. Following drug penetration to the lung tissue, the fraction of drug available to exert the effect depends on the tissue content and drug physicochemical properties, such as lipophilicity, solubility, tissue protein binding, and acidity [36, 37]. Therefore, accounting for fraction unbound in tissue for predictions of the PK/PD relationship may be important [34]. In this work, we did not directly correct site-of-action exposures for protein or tissue binding processes as uncertainty exists in the overall impact of these parameters on the PK/PD relationship for bedaquiline and pretomanid. Evaluations of these relationships may be of interest in future studies.

Our mPBPK models were calibrated to mice PK data. The models were translated to TB patients using allometric scaling and were compared and qualified against dose-ranging plasma concentration data from clinical studies. Although our translational models provided reasonable agreement with the observed plasma concentration data for all three drugs, this work did not include evaluations of best structural model fit to the clinical data, or estimation of individual parameter estimation. The sensitivity analysis identified the most sensitive parameters. Future work may consider estimation of individual parameters using the mPBPK model structure, including further evaluations of the role of the sensitive parameters on exposure using clinical data. Mechanistic understanding included in the mPBPK construct combined with Bayesian estimation using our final parameter estimates as priors may provide a thorough understanding of individual variability and covariate/parameter relationships towards the goal of treatment optimization, especially against persisting Mtb.

Although the validation of our translational approach for predictions of lesion and lung concentrations using pyrazinamide give confidence in the applied approach, our model predictions for lesion and lung concentrations for bedaquiline and pretomanid cannot be compared with observed data from TB patients as such data are not available to date. Our

models may be further validated or further developed in the future when such data are available. In general, the current construct of mPBPK models for bedaquiline and pretomanid are relevant for our primary objective, i.e., to predict exposures in the lungs and lesions of TB patients using preclinical data. Additionally, the good performance of our translational mPBPK approach for pyrazinamide gives confidence that similar translational performance may be expected for other drugs, such as bedaquiline and pretomanid.

## 5 Conclusion

We present the first translational mPBPK models for bedaquiline and pretomanid allowing comprehensive predictions of lung and lesion exposures in patients. Both extensive and continuation phases of current standard bedaquiline dosing were predicted to achieve target exposures within lungs and cavitary lesions to elicit bactericidal activity against replicating bacteria; however, only extensive phase treatment was predicted to achieve target exposures to elicit minimum bactericidal activity against non-replicating bacteria. Standard pretomanid dosing was predicted to achieve target exposures to elicit bactericidal activity against replicating bacteria but not against non-replicating bacteria for most patients. These models can also be further developed to be combined with PD, efficacy, or safety measures to optimize or individualize combination treatment strategies.

**Supplementary Information** The online version contains supplementary material available at <https://doi.org/10.1007/s40262-023-01217-7>.

## Declarations

**Funding** No funding was received for this work.

**Conflicts of interest** Piet H. van der Graaf is an employee of Certara, UK. Krina Mehta, Tingjie Guo, and J.G.C. van Hasselt declare no conflicts of interest.

**Ethics approval** Not applicable.

**Consent to participate** Not applicable.

**Consent for publication** All authors provided consent for publication.

**Availability of data and material** All data used in the analysis were obtained from either the literature (as cited) or from the TB-PACTS database (<https://c-path.org/programs/tb-pacts/>).

**Code availability** Final model codes are provided in the ESM.

**Author contributions** All authors contributed to the study conception and design. KM performed the analysis and wrote the first draft of the manuscript. All authors reviewed and edited the manuscript, and reviewed and approved the final version.

**Open Access** This article is licensed under a Creative Commons Attribution-NonCommercial 4.0 International License, which permits any non-commercial use, sharing, adaptation, distribution and reproduction in any medium or format, as long as you give appropriate credit to the original author(s) and the source, provide a link to the Creative Commons licence, and indicate if changes were made. The images or other third party material in this article are included in the article's Creative Commons licence, unless indicated otherwise in a credit line to the material. If material is not included in the article's Creative Commons licence and your intended use is not permitted by statutory regulation or exceeds the permitted use, you will need to obtain permission directly from the copyright holder. To view a copy of this licence, visit <http://creativecommons.org/licenses/by-nc/4.0/>.

## References

1. World Health Organization. Consolidated operational guidelines on handbook tuberculosis. Geneva: World Health Organization; 2020. p. 132.
2. Khoshnood S, Goudarzi M, Taki E, Darbandi A, Kouhsari E, Heidary M, et al. Bedaquiline: current status and future perspectives. *J Glob Antimicrob Resist*. 2021;25:48–59. <https://doi.org/10.1016/j.jgar.2021.02.017>.
3. Stancil SL, Mirzayev F, Abdel-Rahman SM. Profiling pretomanid as a therapeutic option for tb infection: evidence to date. *Drug Des Devel Ther*. 2021;15:2815–30.
4. Conradie F, Diacon AH, Ngubane N, Howell P, Everitt D, Crook AM, et al. Treatment of highly drug-resistant pulmonary tuberculosis. *N Engl J Med*. 2020;382(10):893–902.
5. Sarathy JP, Dartois V. Caseum: a Niche for *Mycobacterium tuberculosis* drug-tolerant persisters. *Clin Microbiol Rev*. 2020;33(3):e00159-19.
6. Ernest JP, Strydom N, Wang Q, Zhang N, Nuermberger E, Dartois V, et al. Development of new tuberculosis drugs: translation to regimen composition for drug-sensitive and multidrug-resistant tuberculosis. *Annu Rev Pharmacol Toxicol*. 2021;61:495–516.
7. Ordonez AA, Wang H, Magombedze G, Ruiz- CA, Srivastava S, Chen A, et al. Heterogeneous drug exposures in pulmonary lesions. *HHS Public Access*. 2020;26(4):529–34.
8. Kjellsson MC, Via LE, Goh A, Weiner D, Low KM, Kern S, et al. Pharmacokinetic evaluation of the penetration of antituberculosis agents in rabbit pulmonary lesions. *Antimicrob Agents Chemother*. 2012;56(1):446–57.
9. Strydom N, Gupta SV, Fox WS, Via LE, Bang H, Lee M, et al. Tuberculosis drugs' distribution and emergence of resistance in patient's lung lesions: a mechanistic model and tool for regimen and dose optimization. *PLoS Med*. 2019;16(4):e1002773.
10. Dooley KE, Rosenkranz SL, Conradie F, Moran L, Hafner R, von Groote-Bidlingmaier F, et al. QT effects of bedaquiline, delamanid, or both in patients with rifampicin-resistant tuberculosis: a phase 2, open-label, randomised, controlled trial. *Lancet Infect Dis*. 2021;21(7):975–83. [https://doi.org/10.1016/S1473-3099\(20\)30770-2](https://doi.org/10.1016/S1473-3099(20)30770-2).
11. Cohen K, Maartens G. A safety evaluation of bedaquiline for the treatment of multi-drug resistant tuberculosis. *Expert Opin Drug Saf*. 2019;18(10):875–82. <https://doi.org/10.1080/14740338.2019.1648429>.
12. Tanneau L, Karlsson MO, Rosenkranz SL, Cramer YS, Shenje J, Upton CM, et al. Assessing prolongation of the corrected QT interval with bedaquiline and delamanid coadministration to predict the cardiac safety of simplified dosing regimens. *Clin Pharmacol Ther*. 2022;112(4):873–81.

13. US FDA, Center For Drug Evaluation and Research. Center for Drug Evaluation and Research Application Number: 211810Orig1s000: multi-discipline review. US FDA; 2016. pp. 1–264. [https://www.accessdata.fda.gov/drugsatfda\\_docs/nda/2019/212862Orig1s000MultidisciplineR.pdf](https://www.accessdata.fda.gov/drugsatfda_docs/nda/2019/212862Orig1s000MultidisciplineR.pdf).
14. Jermain B, Hanafin PO, Cao Y, Lifschitz A, Lanusse C, Rao GG. Development of a minimal physiologically-based pharmacokinetic model to simulate lung exposure in humans following oral administration of Ivermectin for COVID-19 drug repurposing. *J Pharm Sci.* 2020;109(12):3574–8.
15. Brown RP, Delp MD, Lindstedt SL, Rhomberg LR, Beliles RP. Physiological parameter values for physiologically based pharmacokinetic models. *Toxicol Ind Health.* 1997;13(4):407–84.
16. Ngwalelo P, Brust JCM, van Beek SW, Wasserman S, Maartens G, Meintjes G, et al. Relationship between plasma and intracellular concentrations of bedaquiline and its m2 metabolite in South African patients with rifampin-resistant tuberculosis. *Antimicrob Agents Chemother.* 2021;65:11.
17. Tanneau L, Svensson EM, Rossenu S, Karlsson MO. Exposure–safety analysis of QTc interval and transaminase levels following bedaquiline administration in patients with drug-resistant tuberculosis. *CPT Pharmacometrics Syst Pharmacol.* 2021;10(12):1538–49.
18. Gobburu JVS, Tammara V, Lesko L, Jhee SS, Sramek JJ, Cutler NR, et al. Pharmacokinetic-pharmacodynamic modeling of rivastigmine, a cholinesterase inhibitor, in patients with Alzheimer's disease. *J Clin Pharmacol.* 2001;41(10):1082–90.
19. Chen RY, Yu X, Smith B, Liu X, Gao J, Diacon AH, et al. Radiological and functional evidence of the bronchial spread of tuberculosis: an observational analysis. *Lancet Microbe.* 2021;2(10):e518–26. [https://doi.org/10.1016/S2666-5247\(21\)00058-6](https://doi.org/10.1016/S2666-5247(21)00058-6).
20. Mahmood I, Balian JD. The pharmacokinetic principles behind scaling from preclinical results to phase I protocols. *Clin Pharmacokinet.* 1999;36(1):1–11.
21. Irwin SM, Prideaux B, Lyon ER, Zimmerman MD, Brooks EJ, Schrupp CA, et al. Bedaquiline and pyrazinamide treatment responses are affected by pulmonary lesion heterogeneity in mycobacterium tuberculosis infected C3HeB/FeJ mice. *ACS Infect Dis.* 2016;2(4):251–67.
22. Prideaux B, Via LE, Zimmerman MD, Eum S, Sarathy J, O'Brien P, et al. The association between sterilizing activity and drug distribution into tuberculosis lesions. *Nat Med.* 2015;21(10):1223–7.
23. Rouan MC, Lounis N, Gevers T, Dillen L, Gilissen R, Raouf A, et al. Pharmacokinetics and pharmacodynamics of TMC207 and its N-desmethyl metabolite in a murine model of tuberculosis. *Antimicrob Agents Chemother.* 2012;56(3):1444–51.
24. Ahmad Z, Peloquin CA, Singh RP, Derendorf H, Tyagi S, Ginsberg A, et al. PA-824 exhibits time-dependent activity in a murine model of tuberculosis. *Antimicrob Agents Chemother.* 2011;55(1):239–45.
25. Mota F, Ruiz-Bedoya C, Tucker E, De Jesus P, Flavahan K, Turner M, et al. Noninvasive assessment of intralesional antimicrobial concentration-time profiles in pulmonary and central nervous system tuberculosis using dynamic 18F-pretomanid positron emission tomography. *Open Forum Infect Dis.* 2021;8(Suppl 1):S789–90. <https://doi.org/10.1093/ofid/ofab466.1603>.
26. Ismail NA, Omar SV, Joseph L, Govender N, Blows L, Ismail F, et al. Defining bedaquiline susceptibility, resistance, cross-resistance and associated genetic determinants: a retrospective cohort study. *EBioMedicine.* 2018;28:136–42. <https://doi.org/10.1016/j.ebiom.2018.01.005>.
27. van Heeswijk RPG, Dannemann B, Hoetelmans RMW. Bedaquiline: a review of human pharmacokinetics and drug-drug interactions. *J Antimicrob Chemother.* 2014;69(9):2310–8.
28. Diacon AH, Dawson R, Von Groote-Bidlingmaier F, Symons G, Venter A, Donald PR, et al. Bactericidal activity of pyrazinamide and clofazimine alone and in combinations with pretomanid and bedaquiline. *Am J Respir Crit Care Med.* 2015;191(8):943–53.
29. Chesov E, Chesov D, Maurer FP, Andres S, Utpatel C, Barilar I, et al. Emergence of bedaquiline resistance in a high tuberculosis burden country. *Eur Respir J.* 2022;59(3):1–10. <https://doi.org/10.1183/13993003.00621-2021>.
30. Allué-Guardia A, Garcia-Vilanova A, Olmo-Fontán AM, Peters J, Maselli DJ, Wang Y, et al. Host- and age-dependent transcriptional changes in *Mycobacterium tuberculosis* cell envelope biosynthesis genes after exposure to human alveolar lining fluid. *Int J Mol Sci.* 2022;23(2). <https://www.mdpi.com/1422-0067/23/2/983>
31. Drusano GL, Kim S, Almoslem M, Schmidt S, D'Argenio DZ, Myrick J, et al. The funnel: a screening technique for identifying optimal two-drug combination chemotherapy regimens. *Antimicrob Agents Chemother.* 2021;65:2.
32. Jarugula P, Scott S, Ivaturi V, Noack A, Moffett BS, Bhutta A, et al. Understanding the role of pharmacometrics-based clinical decision support systems in pediatric patient management: a case study using Lyv software. *J Clin Pharmacol.* 2021;61(Suppl 1):S125–32.
33. Hughes JH, Tong DMH, Lucas SS, Faldasz JD, Goswami S, Keizer RJ. Continuous learning in model-informed precision dosing: a case study in pediatric dosing of vancomycin. *Clin Pharmacol Ther.* 2021;109(1):233–42.
34. Humphries H, Almond L, Berg A, Gardner I, Hatley O, Pan X, et al. Development of physiologically-based pharmacokinetic models for standard of care and newer tuberculosis drugs. *CPT Pharmacometrics Syst Pharmacol.* 2021;10(11):1382–95.
35. Cao Y, Jusko WJ. Applications of minimal physiologically-based pharmacokinetic models. *J Pharmacokinet Pharmacodyn.* 2012;39(6):711–23.
36. Rowland M, Tozer TN. *Clinical pharmacokinetics and pharmacodynamics: concepts and applications*; 1980.
37. Shargel L, Wu-Pong S, Yu ABC. Chapter 10. physiologic drug distribution and protein binding. In: *Applied biopharmaceutics and pharmacokinetics*, 6e. New York: The McGraw-Hill Companies; 2012. <http://accesspharmacy.mhmedical.com/content.aspx?aid=56603200>.
38. Diacon AH, Dawson R, von Groote-Bidlingmaier F, Symons G, Venter A, Donald PR, et al. 14-day bactericidal activity of PA-824, bedaquiline, pyrazinamide, and moxifloxacin combinations: a randomised trial. *Lancet.* 2012;380(9846):986–93.
39. The global alliance for tb drug development. Evaluation of Early Bactericidal Activity in Pulmonary Tuberculosis (TMC207-CL001). 2017. <https://clinicaltrials.gov/show/NCT01215110>.
40. Kim S, Yamada WM, Duncanson B, Nole J, Rogers S, Parker S, et al. Building optimal three-drug combination chemotherapy regimens to eradicate mycobacterium tuberculosis in its slow-growth acid phase. *Antimicrob Agents Chemother.* 2021;65(10):e00693-e721. <https://doi.org/10.1128/AAC.00693-21>.
41. Lyons MA. Pretomanid dose selection for pulmonary tuberculosis: an application of multi-objective optimization to dosage regimen design. *CPT Pharmacometrics Syst Pharmacol.* 2021;10(3):211–9.
42. Muliaditan M, Della PO. Evaluation of pharmacokinetic–pharmacodynamic relationships and selection of drug combinations for tuberculosis. *Br J Clin Pharmacol.* 2021;87(1):140–51.